PHYSICAL REVIEW A **72**, 031801(R) (2005)

Tunable whispering-gallery-mode resonators for cavity quantum electrodynamics

Y. Louyer, D. Meschede, and A. Rauschenbeutel*
Institut für Angewandte Physik, Universität Bonn, Wegelerstrasse 8, D-53115 Bonn, Germany
(Received 31 December 2004; published 15 September 2005)

We theoretically study the properties of highly prolate-shaped dielectric microresonators. Such resonators sustain whispering-gallery modes that exhibit two spatially well-separated regions with enhanced field strength. The field per photon on the resonator surface is significantly higher than, e.g., for equatorial whispering-gallery modes in microsphere resonators with a comparable mode volume. At the same time, the frequency spacing of these modes is much more favorable, so that a tuning range of several free spectral ranges should be attainable. We discuss the possible application of such resonators for cavity quantum electrodynamics experiments with neutral atoms and reveal distinct advantages with respect to existing concepts.

DOI: 10.1103/PhysRevA.72.031801 PACS number(s): 42.55.Sa, 03.65.Ge, 42.50.Pq

Optical microresonators have attracted much interest in the field of linear and nonlinear optics as well as in cavity quantum electrodynamics (CQED), as summarized in the recent review by Vahala [1]. One of the reasons for this considerable attention is the prime importance of a small mode volume V for such applications. So far, optical microresonators based on Fabry-Perot cavities, photonic crystals, and whispering-gallery modes have been realized [1]. In addition to V, certain applications, such as cavity quantum electrodynamics [2], require also a minimization of the ratio V/Q, where the quality factor Q is determined by the energy storage time in units of the optical period.

Very high Q values have been realized for Fabry-Perot cavities with ultrahigh reflectance mirrors [3]. However, the mirror components are involved and costly to manufacture. Furthermore, due to the modular construction, such resonators require an elaborate active stabilization of their resonance frequency. Photonic crystal-based resonators have a much better passive stability and yield extremely small mode volumes. Even though the experimentally realized Q values fall well below the theoretical limits, they reach record values for V/Q [4]. However, the problem of tuning the resonance frequency of such structures remains.

The highest Q-values for optical resonators to date have been realized with whispering-gallery modes (WGMs) in fused silica microspheres and microtori [5,6], where continuous total internal reflection confines the light to a thin "equatorial" ring near the surface of the resonator. In combination with their relatively small mode volume of $V \approx 1000\,\lambda^3$, where λ is the optical wavelength, these modes are therefore ideal candidates for CQED experiments.

Optical probing and output coupling requires phase matching of the WGMs to propagating light fields. This has been achieved with various methods, all of which use auxiliary dielectric structures (prisms [7], eroded or tapered optical fibers [8,9], or fiber-prism hybrid systems [10]) that are introduced into the external evanescent field of the WGM in the vicinity ($\lesssim\lambda$) of the resonator surface. Using such a setup, strong coupling between atoms in a dilute vapor and a microsphere WGM has been realized [11]. However, in spite of considerable research activities, a *controlled* strong coupling of a suitable dipole emitter to a WGM has not yet been accomplished. The main experimental difficulty consists in controllably placing the emitter as close as possible to the dielectric surface. In particular, due to the two-dimensional character of equatorial WGMs, the prism or fiber coupler severely limits the mechanical and optical access.

Another critical issue is tunability. For a $\varnothing \approx 75\ \mu$m diameter equatorial WGM, tuning over one free spectral range (FSR) requires a change of the optical path length of about 3×10^{-3}. Electrical thermo-optic tuning of a $\varnothing \approx 75\ \mu$m microtorus over up to 30% of a FSR has been demonstrated [12]. It relies on the temperature dependence of the refractive index of silica, $\partial n/\partial T \approx 1.3 \times 10^{-5}\ \mathrm{K}^{-1}$. Another solution for tuning is to elastically deform the resonator through mechanical strain. For a $\varnothing \approx 80\ \mu$m microsphere, tuning over 50% of an FSR has been achieved with this method, limited by the mechanical damage threshold of the resonator setup [13]. Finally, it should be noted that for a $\varnothing \approx 50\ \mu$m equatorial WGM with $Q \approx 10^9$ the resonance linewidth is only 10^{-7} of a FSR. Therefore, even if a tuning device reached a full FSR tuning range, it would be a challenging task to guarantee the corresponding passive stability.

Here, we propose the use of WGMs in highly prolate dielectric resonators with a cylindrical symmetry. Of course, such a structure also sustains "equatorial" WGMs, i.e., with a corresponding ray path that is closed after one revolution around the resonator axis. In the following, however, we will consider modes for which the light spirals back and forth along the resonator axis between two turning points, separated by $2z_c$ (see Fig. 1).

From this very simple ray path picture it is already apparent that such modes exhibit two spatially separated caustics located at $\pm z_c$ with an enhanced field strength. Note that, in analogy to a charged particle in a magnetic bottle, the light is in fact confined along the z axis between the two turning points by an angular momentum barrier. For this reason, we have adopted the denomination "bottle modes" from Ref. [14], where such a resonator shape was theoretically constructed from an equidistant spectrum of eigenmodes using a WKB approximation.

We will now present a full-scale wave equation calcula-

*Electronic address: rauschenbeutel@iap.uni-bonn.de

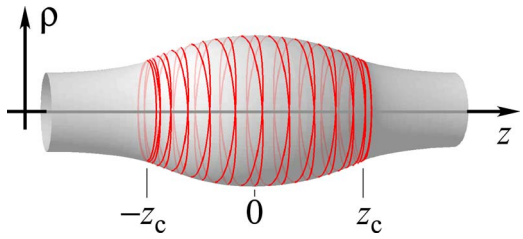

FIG. 1. (Color online) Sketch of the resonator geometry. The ray path corresponding to the whispering-gallery modes under consideration is schematically indicated. Note that the thickness variation of the resonator structure along the z axis is amplified for illustration purposes.

tion for such a resonator shape and theoretically explore important resonator properties, including field distribution, mode volume, and tunability. We consider a resonator profile that is approximately parabolic along z

$$R(z) \approx R_0\left(1 - \frac{1}{2}(\Delta k z)^2\right), \tag{1}$$

where we take $R_0 \approx 8\ \mu$m as the maximal radius and $\Delta k^2 \approx 10^{-5}\ \mu\text{m}^{-2}$ for the curvature of the profile. We use the method of adiabatic invariants [15], well known from the description of the dynamics in magnetic bottles. Indeed, due to the small variation of the resonator radius (amplified in Fig. 1), $dR/dz \ll 1$, and since we are considering maximum angular momentum modes located close to the surface of the resonator, the radial component k_ρ of the wave vector is negligible with respect to k_z and k_φ. Therefore, the total wave number is

$$k = (k_z^2 + k_\varphi^2)^{1/2} = 2\pi n/\lambda, \tag{2}$$

where n and λ are the effective index of refraction and the wavelength in vacuum, respectively. Now, due to cylindrical symmetry, the projection of the angular momentum onto the z axis is a conserved quantity, $\partial_z k_\varphi(z)R(z) = 0$. Furthermore, the axial component of the wave vector vanishes in the caustics, $k_z(\pm z_c) = 0$, so that $k_\varphi(\pm z_c) = k$. The azimuthal and axial components of the wave vector thus read

$$k_\varphi(z) = kR_c/R(z), \tag{3}$$

$$k_z(z) = \pm k\sqrt{1 - [R_c/R(z)]^2}, \tag{4}$$

where $-z_c \leqslant z \leqslant z_c$ and $R_c = R(z_c)$.

In order to check that the paraxial approximation of a negligible radial wave-vector component is well justified for the resonator geometry of Eq. (1), we use the relation $k_\rho = (dR/dz)k_z$. For $z_c \approx 80\ \mu$m this yields $|k_\rho(z)| < 6 \times 10^{-3}|k_z(z)|$ in the region $-z_c \leqslant z \leqslant z_c$. Inserting this value as a correction into Eq. (2), we estimate the error in Eq. (4) to be smaller than 2×10^{-5}.

Using the adiabatic approximation, we will now establish the wave equation and determine the eigenfunctions of the resonator. Due to the cylindrical symmetry, the azimuthal part of the wave equation can be separated with solutions proportional to $\exp(im\varphi)$, where m is the azimuthal quantum number. The solution can thus be written $\Psi(\rho,z)\exp(im\varphi)$. The radial quantum number p will be fixed to its minimum value $p=1$, corresponding to modes located at the surface of the resonator. Now, using the adiabatic approximation along the z axis, $\Psi(\rho,z)$ can be separated in a product of two functions $\Phi(\rho,z)Z(z)$, where Φ is the solution of a Bessel equation,

$$\frac{\partial^2\Phi}{\partial\rho^2} + \frac{1}{\rho}\frac{\partial\Phi}{\partial\rho} + \left(k_\varphi^2 - \frac{m^2}{\rho^2}\right)\Phi = 0. \tag{5}$$

Here, k_φ is given by Eq. (3) and, using $kR_c = m$, equals $k_\varphi(z) = m/R(z)$. Insertion into the above equation yields

$$\frac{\partial^2\Phi}{\partial\rho^2} + \frac{1}{\rho}\frac{\partial\Phi}{\partial\rho} + m^2\left(\frac{1}{R(z)^2} - \frac{1}{\rho^2}\right)\Phi = 0. \tag{6}$$

In order to determine the radial wave function from this equation, we fix the boundary conditions at the resonator surface such that Φ and its derivative $\partial\Phi/\partial\rho$ be continuous, thereby assuming linear polarization with the electric field parallel to the resonator surface. This approximation is well justified for our geometry and leads to analytic solutions. Determining the exact modes including polarization would require a numerical finite element calculation. The solution of Eq. (6) can be written

$$\Phi_m(\rho,z) = \begin{cases} A_m J_m(k_\varphi\rho) & [\rho < R(z)] \\ H_m^{(2)}\left(\frac{k_\varphi\rho}{n}\right) + S_m H_m^{(1)}\left(\frac{k_\varphi\rho}{n}\right) & [\rho > R(z)] \end{cases}, \tag{7}$$

where j_m and $H_m^{(1,2)}$ are the Bessel and Hankel functions, respectively. The coefficients A_m and S_m are determined such that the boundary conditions are satisfied.

The differential equation for Z also depends on the resonator profile $R(z)$. In order to find an analytic solution, we choose the explicit form $R(z) = R_0/\sqrt{1+(\Delta k z)^2}$, which, given that $(\Delta k z)^2 < 0.05$ in our case, realizes the parabolic profile of Eq. (1) to a very good approximation. Using this form, the problem reduces to a simple harmonic oscillator,

$$\frac{\partial^2 Z}{\partial z^2} + \left(k^2 - \frac{m^2}{R_0^2} - \frac{m^2\Delta k^2}{R_0^2}z^2\right)Z = 0. \tag{8}$$

In analogy to the harmonic oscillator problem, we can therefore identify the total and the potential energy as $E = k^2 - m^2/R_0^2$ and $V(z) = (\Delta E_m z/2)^2$, respectively, where we have set $\Delta E_m = 2m\Delta k/R_0$. Furthermore, the condition that Z be square integrable leads to a discrete set of energy levels $E_{mq} = (q+1/2)\Delta E_m$, where q is the axial quantum number, corresponding to the number of nodes of the wave function along z. This allows us to deduce the allowed eigenvalues

$$k_{mq} = [m^2/R_0^2 + (q+1/2)\Delta E_m]^{1/2}, \tag{9}$$

with the corresponding solution of Eq. (8),

$$Z_{mq}(z) = C_{mq}H_q\left(\sqrt{\frac{\Delta E_m}{2}}z\right)\exp\left(-\frac{\Delta E_m}{4}z^2\right), \tag{10}$$

where H_q is the Hermite polynomial of order q with the normalization constant $C_{mq} = [\Delta E_m/(\pi 2^{2q+1}(q!)^2)]^{1/4}$.

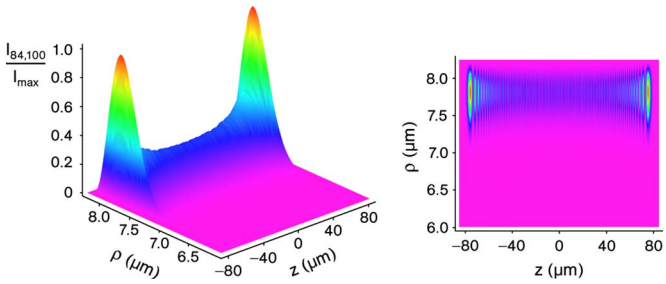

FIG. 2. (Color online) Intensity distribution of the bottle mode.

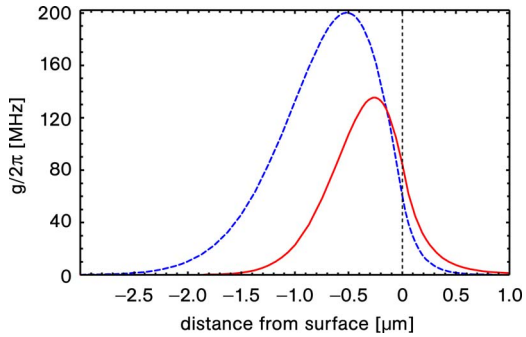

FIG. 3. (Color online) Coupling strength of a Cs atom to the mode of the bottle resonator as a function of the distance from the resonator surface (solid line). The atom is placed at the point of highest field intensity along the resonator axis, $z=z_c$. For comparison, the coupling to an equatorial WGM of a $\varnothing=50$ μm microsphere is also given (dashed line). Due to its smaller mode volume, the maximum coupling coefficient for the microsphere is a factor of 1.4 larger. However, the coupling at the resonator surface is 1.5 times larger for the bottle resonator, because its evanescent field is more pronounced.

From the wave function $\Psi_{mq}(\rho,z)=\Phi_m(\rho,z)Z_{mq}(z)$ we can now calculate the intensity distribution $I_{mq}(\rho,z) \propto |\Psi_{mq}(\rho,z)|^2$ of the bottle modes. We consider the case where the wavelength λ_{mq} matches the $D2$ line of Cs at 852 nm. We choose the resonator radius at the caustics to be $R_c=7.8$ μm, compatible with a quality factor of $Q\approx 10^9$ [16]. Moreover, we set $n=1.467$, $\Delta k=0.0032$ μm^{-1}, $q=100$, and $m=84$, i.e., the highest possible m value. Figure 2 shows $I_{mq}(\rho,z)$ for the corresponding bottle mode. The intensity in the caustics, located at $z_c=\pm 77.3$ μm, is enhanced by a factor of four compared to the peak value around $z=0$.

The intensity distribution directly yields the mode volume V of the bottle modes. It is obtained by normalizing $I_{mq}(\rho,z)$ to unity and by integrating it according to

$$V_{mq}=\int\int\int_0^{\rho_0(z)} \varepsilon(\rho,z)\frac{I_{mq}(\rho,z)}{I_{mq}^{\max}}\rho\, d\rho\, d\varphi\, dz, \qquad (11)$$

where $\varepsilon(\rho,z)=n^2$ inside the resonator and 1 outside, n being the index of refraction of the resonator material. The upper limit for the radial integral, $\rho_0(z)$, is chosen such that it coincides with the first zero of the radial wave function outside the resonator, $\Phi_m(\rho_0,z)\equiv 0$, in order to include the effects of the evanescent field. For the bottle mode of Fig. 2 we find $V_{84\ 100}=749$ μm^3. This value is only twice as large as the mode volume of a microsphere with $\varnothing\approx 50$ μm.

Now, the *maximum* coupling strength of a given dipole emitter to a single photon in the resonator mode is inversely proportional to the square root of the mode volume, $g \propto 1/\sqrt{V}$. However, for WGMs we can only access the field outside of the resonator. The actual parameter of interest is therefore the coupling strength at the surface of the resonator. We have calculated this value for our bottle resonator at the position of the caustic z_c. For the $D2$ transition of a Cs atom we find $g/2\pi\approx 90$ MHz. In spite of the larger mode volume, this exceeds the expected coupling strength to the equatorial WGM at the surface of a $\varnothing\approx 50$ μm microsphere by a factor 1.5. The physical reason for this result lies in the fact that, due to the smaller diameter of the bottle resonator, its evanescent field is more pronounced than for the larger microsphere (see Fig. 3).

We now examine the mode spectrum of the bottle resonator, given by Eq. (9). For our geometry, i.e., $R_0\Delta k \ll 1$ and $m\approx q$, one finds that the frequency spacing between modes for which the azimuthal quantum number m differs by one approximately equals $\Delta\nu_m\approx c/2\pi n R_0\approx 4$ THz, just as large as for an equatorial WGM of the same radius. However, the mode spacing concerning the axial quantum number q is much smaller and is given by $\Delta\nu_q\approx c\Delta k/2\pi\approx 150$ GHz, one order of magnitude smaller than for a $\varnothing\approx 50$ μm equatorial WGM. Tuning over one free spectral range therefore only requires a change of the optical path length of 4×10^{-4}. This can be realized by varying the resonator temperature by 30 K, a parameter range that is easily accessible in an experiment.

Mechanical strain could also be used to tune the bottle resonator. Concerning its mechanical properties, we approximate the resonator as a cylinder of radius R_0. This is well justified in our case and allows an easy estimation of the effect of the strain on the mode frequency ν_{mq}. Using the Poisson coefficient and the elasto-optic coefficients of silica [17] and neglecting the modification of the curvature Δk along the resonator axis, we find

$$\Delta\nu_{mq}/\nu_{mq}\approx -\Delta R/R_0-\Delta n/n\approx -0.2\Delta L/L \qquad (12)$$

for the TM mode (polarization parallel to the strain), where L is the length of the resonator. One FSR tuning in our case thus requires a length change of about 2×10^{-3}. Using the value of 7.2×10^{10} Pa for the elasticity module of silica, this implies a strain of about 0.15 GPa, more than one order of magnitude smaller than the typical damage threshold for silica fibers of 3 GPa [18]. Strain tuning over several FSR therefore seems possible.

Apart from the advantageous properties concerning mode volume and tunability, the bottle resonator geometry and the resulting spatial structure of the modes also offer interesting advantages with respect to their handling and possible applications. Contrary to equatorial WGMs, bottle resonators exhibit *two* spatially well-separated regions of enhanced field strength (see Fig. 2) and are thus true two-port devices: One of the two caustics could, e.g., be used to couple light into and out of the resonator by means of a thin unclad optical

fiber [9], while a dipole emitter could be coupled to the other caustic.

In practice, it has been demonstrated that a prolate resonator geometry with the dimensions considered here can be realized on unclad optical fibers using fiber pulling techniques and CO_2 laser microstructuring [19]. In order to obtain the desired high Q values, these processes will have to be optimized to yield a surface quality that minimizes scattering losses. Furthermore, the bulk absorption of the fiber cladding, which would exclusively guide the light in this case, has to be sufficiently low. Using low-loss telecommunication fibers, we are however confident, that this condition can be fulfilled.

Summarizing, we have studied the properties of whispering-gallery modes in highly prolate-shaped silica resonators. We have shown that such "bottle resonators" sustain modes that exhibit two spatially well-separated caustics with an enhanced field strength. For a distance of 155 μm between the caustics and a resonator diameter of 16 μm we find a mode volume of 749 μm^3, only twice as large as for an equatorial whispering gallery mode in a silica microsphere with a diameter of 50 μm. In spite of this larger mode volume, the coupling strength of an atom to the evanescent field of the mode *outside* of the bottle resonator is larger than for a microsphere: Due to the smaller radius of the bottle resonator, its evanescent field is stronger. For the $D2$ transition of Cs, we calculate a coupling strength of $g/2\pi \approx 90$ MHz, much larger than the atomic line width and the expected cavity line width for an estimated quality factor of 10^8 to 10^9. The bottle resonator should therefore allow to enter the strong coupling regime in neutral atom CQED.

At the same time, we have shown that the mode spacing for the bottle resonator is one order of magnitude smaller than for an equatorial WGM with a diameter of 50-μm. By varying the temperature or applying mechanical strain to the resonator, tuning over more than one free spectral range should therefore be possible. Moreover, the fact that bottle resonators are true two-port devices is an important advantage when it comes to probing the light field in the resonator mode while simultaneously coupling a dipole emitter to it. Finally, it has recently been proposed to trap and guide atoms around thin unclad optical fibers using a two-color evanescent light field [20]. Our resonator design seems particularly suited to be combined with such a surface trap in order to couple trapped cold atoms to the resonator mode.

We acknowledge support from the Deutsche Forschungsgemeinschaft in the framework of the research unit 557 "Light Confinement and Control with Structured Dielectrics and Metals" and from the EC in the framework of the Research Training Network "FASTnet."

[1] K. J. Vahala, Nature (London) **424**, 839 (2003).
[2] *Cavity Quantum Electrodynamics*, edited by P. R. Berman (Academic Press, New York, 1994).
[3] G. Rempe, R. J. Thompson, H. J. Kimble, and R. Lalezari, Opt. Lett. **17**, 363 (1992).
[4] Y. Akahane, T. Asano, B.-S. Song, and S. Noda, Nature (London) **425**, 944 (2003).
[5] M. L. Gorodetsky, A. A. Savechenkov, and V. S. Ilchenko, Opt. Lett. **21**, 453 (1996).
[6] D. K. Armani, T. J. Kippenberg, S. M. Spillane, and K. J. Vahala, Nature (London) **421**, 925 (2003).
[7] M. L. Gorodetsky and V. S. Ilchenko, Opt. Commun. **113**, 133 (1994).
[8] A. Serpenguezel, S. Arnold, and G. Griffel, Opt. Lett. **20**, 654 (1995); N. Dubreuil, J. C. Knight, D. Leventhal, V. Sandoghdar, J. Hare, and V. Lefèvre, *ibid.* **20**, 813 (1995).
[9] J. C. Knight, G. Cheung, F. Jacques, and T. A. Birks, Opt. Lett. **22**, 1129 (1997).
[10] V. S. Ilchenko, X. S. Yao, and L. Maleki, Opt. Lett. **24**, 723 (1999).
[11] D. W. Vernooy, A. Furusawa, N. Ph. Georgiades, V. S. Ilchenko, and H. J. Kimble, Phys. Rev. A **57**, R2293 (1998).
[12] D. Armani, B. Min, A. Martin, and K. J. Vahala, Appl. Phys. Lett. **85**, 5439 (2004).
[13] W. von Klitzing, R. Long, V. S. Ilchenko, J. Hare, and Valérie Lefèvre-Seguin, New J. Phys. **3**, 14 (2001).
[14] M. Summetsky, Opt. Lett. **29**, 8 (2004).
[15] I. Percival and D. Richards, *Introduction to Dynamics* (Cambridge University Press, Cambridge, 1982), Sec. 9.4.
[16] J. R. Buck and H. J. Kimble, Phys. Rev. A **67**, 033806 (2003).
[17] N. F. Borrelli and R. A. Miller, Appl. Opt. **7**, 745 (1968).
[18] G. S. Glaesmann and D. J. Walther, Opt. Eng. (Bellingham) **30**, 746 (1991).
[19] G. Karantzas, T. E. Dimmick, T. A. Birks, R. Le Roux, and P. St. J. Russel, Opt. Lett. **26**, 1137 (2001).
[20] Fam Le Kien, V. I. Balykin, and K. Hakuta, Phys. Rev. A **70**, 063403 (2004).